Journal of Computational Information Systems 9: 16 (2013) 6643–6650
Available at http://www.Jofcis.com

Rolling Bearing Failure Feature Extraction Based on Large Parameters Stochastic Resonance*

Zengqiang MA*, Yingna YANG, Sha ZHONG

School of Electrical and Electronics Engineering, Shijiazhuang Tiedao University, Shijiazhuang 050043, China

Abstract

Based on rolling bearing fault signal modulation model in the process of spreading, an improved method that combining Hilbert envelop extraction algorithm and large parameter setting rules in stochastic resonance (SR) is proposed for features extraction. Firstly, Hilbert transform can effectively eliminate the interference of high frequency carrier signal. Secondly, parameters setting rules in a certain frequency range are summarized based on the simulation research on the realization of stochastic resonance under the condition of big parameters. Then, the improved method is used to deal with the experimental data of rolling bearing with typical faults. The experimental results show that the improved method can extract the fault feature and identify the fault type effectively.

Keywords: Rolling Bearing; Hilbert Transform; Envelope Detection; Large Parameters Stochastic Resonance

1 Introduction

Rolling bearings is one of the most commonly used general spare parts in all kinds of rotating machinery. The fault diagnosis from the weak signals have become one of the research focus all over the world [1]. The traditional diagnosis methods usually base on the time domain or frequency domain vibration signals analysis. In recent years, the methods combining time-frequency transform and statistical analysis have gotten rapid development. The representative methods are wavelet packet technology, blind source separation and stochastic resonance. Comparing with the original wavelet algorithms, wavelet packet [2] can perform some more detailed examinations and more flexible time-frequency resolution for the weak signals. But its effectiveness for weak signals analysis strongly depends on the prior experiences. For example, the analysis results of a same signal are different as the different wavelet base functions are used. Blind source separation [3, 4] is another good method to separating the original signal from noise as the prior knowledge and the training data be gained in advance. Nonetheless, the method of blind source separation

*Project supported by National Natural Science Funds of China Key Program (No. 11227201), National Natural Science Foundation of China (No. 11202141).

*Corresponding author.
Email address: mzqlunwen@126.com (Zengqiang MA).

1553–9105 / Copyright © 2013 Binary Information Press
DOI: 10.12733/jcisP0771
August 15, 2013

doesn't work well as the signal source number is unknown or the signal can't fully satisfy the constraint conditions [5]. Stochastic resonance (SR) is also a common method of extracting the fault features from the weak signal [6]. It is a kind of nonlinear phenomenon: when the original signal and the noise, which are put into the SR system, match the SR system to some extent, some noise energy will be transferred to the periodic signal and the signal-to-noise ratio of the output signals will be rising to the peak. However, the SR method is restricted to be used under the condition of adiabatic approximation [6], just the low frequency small parameter, which is much less than that of the signals acquired in practical engineering application.

In order to overcome the limitation of the adiabatic approximation and promote its applications in the fields of fault feature extraction, an improved method that combined with the Hilbert transform [7] and the large parameter SR algorithm is proposed based on the rolling bearing modulation model in this paper. In addition, the large parameter setting rules are also put forward in certain frequency range based on a serial of simulation experiments. Then the improved method and the large parameter setting rules are used to diagnose three typical faults of rolling bearings. The experiment results show that obvious peaks appear at fault features frequency and the signal-to-noise ratio of the useful signal has been increased dramatically.

2 Principle of the Improved Method for Fault Feature Extraction

2.1 Rolling bearing fault signal modulation model

Rolling bearing is a kind of high precision parts. It can generate two kinds of vibrations in the normal operation. One is normal vibration, the other is natural vibration. Natural vibration has a large natural frequency at 1∼20KHz, and sometimes up to 80KHz [8]. Once some local damage appears in rolling bearing, periodic collision will occurs on contact surface with other components, which is called through vibration (fault vibration). When rolling bearing faults happen, the actual collected vibration signal always contains normal vibration and natural vibration. Various kinds of signals produced by different vibration sources are relatively independent. They are mixed and superimposed into the measured vibration signal by way of multiplication or plus, whose multi-mixed mechanism is similar to amplitude modulation. Because the natural vibration signal has the largest amplitude and frequency, the rolling bearing modulation model can be simplified as follows:

$$s(t) = A(1 + \sum_{i=1}^{k} r_i sin(2\pi f_i t + \theta_i))sin(2\pi f_r t + \varphi) + n(t) \quad (1)$$

where f_i is the fault features frequency or other ingredient, f_r is the natural frequency, $Asin(2\pi f_r t + \varphi)$ is a modulation signal, and $r_i sin(2\pi f_i t + \theta_i)$ is high frequency natural oscillation carrier signal.

Based on the above rolling bearing modulation model, Fig. 1 is a block diagram of fault feature extraction, and the part in dotted line box is the improved method proposed in the paper.

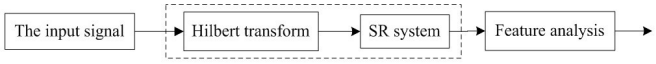

Fig. 1: Principle of the improved method for fault feature extraction

2.2 Hilbert envelope detection principle

Hilbert transform has the many advantages, such as excellent envelope detection ability, good adaptability and high feature extraction accuracy as the high frequency carrier signal is unknown. It can be used to eliminate the interference of high frequency noise. Suppose $x(t)$=$b(t)g(t)$, $g(t)$ is the high frequency signal, and $b(t)$ is the low frequency signal, the Hilbert transfer of $x(t)$ is as follows:

$$\hat{x}(t) = b(t)\hat{g}(t) \tag{2}$$

The above Eq. (2) [9] descripts that if a low frequency signal multiplies a high frequency signal, the latter one plays a leading role in Hilbert transformation of their product term. As a hypothesis, non-noise part in rolling bearing vibration model is shown by Eq. (3):

$$s_1(t) = A(1 + \sum_{i=1}^{k} r_i sin(2\pi f_i t + \theta_i))sin(2\pi f_r t + \varphi) \tag{3}$$

Depending on Eq. (2), the Hilbert transformation of $s_1(t)$ can be worked out as follows:

$$s_1(t) = A(1 + \sum_{i=1}^{k} r_i sin(2\pi f_i t + \theta_i))cos(2\pi f_r t + \varphi) \tag{4}$$

$$|\hat{s_1}(t)| = \sqrt{s_1(t)^2 + \hat{s_1}(t)^2} = \left| A(1 + \sum_{i=1}^{k} r_i sin(2\pi f_i t + \theta_i)) \right| \tag{5}$$

As seen, $|\hat{s_1}(t)|$ in Eq. (5) is the signal envelop that comprises all kinds of fault features according to Eq. (1). From Eq. (3) to Eq. (5), it is demonstrated that high frequency part can be eliminated from the modulated model through Hilbert transformation, and the low frequency envelope containing fault features can be separated without damaging the original signal. Of course, this is the ideal result without noises. In fact, the signal frequency spectrum after Hilbert transformation still contains other frequency components, and the features of fault are not evident yet. So it is needed to use SR to making a further operating and extracting the fault features.

2.3 Principle of the improved SR

SR algorithm can highlight the periodic signal from an input signal mixed with noise and enhance signal-to-noise ratio (SNR) of the output. Double steady-state system is a typical SR. The Langevin equation of Eq. (6) is the typical model to describe double steady-state nonlinear system.

$$\frac{dx}{dt} = ax - bx^3 + s(t) + n(t) \tag{6}$$

In Eq. (6), $x(t)$ is the system output; $s(t)$ is input signal of the nonlinear systems, and $n(t)$ is random noise signal. Because of the adiabatic condition (low frequency small parameter), the original SR system is not satisfied for most of the actual signals. A variable step algorithm [10] is used to realize the large parameter SR in the improved method.In the solving process, the change of parameters make a huge impact on the output. To clearly observe the influence on output by parameters changing, this paper defines a new variable A_{psd}:

$$A_{psd} = (\frac{O_{psd}}{I_{psd}})_{f=f_0} \tag{7}$$

O_{psd} and I_{psd} are respectively output power spectrum value and input signal power spectrum value of SR at the periodic signal frequency.

In Eq. (6), suppose that $s(t)$=$Asin(2\pi f_0 t)$ and noise variance of $n(t)$ is D. f_s is sampling frequency, and h is difference iteration step length. Tab. 1 show results that are figured out under different parameter values. As seen, A_{psd} declines with the increase of f, but its value is always more than two. So the obvious phenomenon of SR can be obtained under the condition of large frequency through adjusting variable step length and parameters values.

Table 1: Parameters adjustment list of SR under different signal frequency

f/Hz	f_s/Hz	h	a	b	A	D	A_{psd}
0.01	5	0.2	1	1	0.3	0.6	11.124573
0.1	50	0.02	0.6	1	0.3	0.6	8.5211374
1	500	0.02	0.4	1	0.3	0.6	6.4888122
10	5000	0.02	0.3	1	0.3	0.6	5.6229949
50	25000	0.02	0.3	1	0.3	0.6	2.3423976
100	50000	0.02	0.2	1	0.3	0.6	2.5345462
500	250000	0.02	0.2	1	0.3	0.6	2.4079289

3 Large Parameter Setting Rules in SR

According to the information in Tab. 1, a conclusion can be drawn that the parameters variation of f_s, h, a and b have effects on the performance of the large parameter SR. Therefore, it is necessary to study and summarize the large parameter setting rules in SR. The sampling frequency is respectively set at f=10Hz and f=100Hz. Initial parameter values of $s(t)$ and $n(t)$ are set as shown in Tab. 1.

3.1 Operation parameter setting rules of f_s and h

In Fig. 2(a), the power spectral gain at the periodic signal frequency of A_{psd} roughly heightens linearly with the increase of f_s.

(1) When $f_s/f = 300$, $A_{psd} = 1$.

(2) When $f_s/f < 300$, $A_{psd} < 1$. Periodic signal energy is weakened after the SR system.

(3) When $f_s/f > 300$, $A_{psd} > 1$. Periodic signal energy is enhanced after the SR system. The system has the de-noising effect.

Although raise of f_s can contribute to improve the performance effect of the SR system, he higher requirement for calculating ability of computer hardware is needed in practical application. So it is suggested taking $f_s/f \geq 300$.

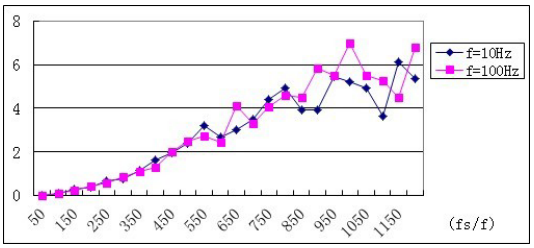

(a) The changing curve of A_{psd} with f_s

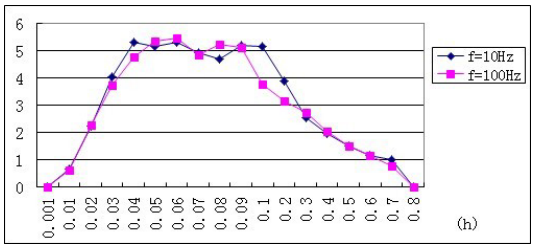

(b) The changing curve of A_{psd} with h

Fig. 2: The changing curve of A_{psd} with operation parameter at f=10Hz and f=100Hz

Step of h is usually assigned as h=$\frac{1}{f_s}$ [11]. Fig. 2(b) show the changing curve A_{psd} of with h at f_s/f=500. When the value of h is too large or too small, A_{psd} will shape declines. When h is assigned a value in $(0.15, 0.6)$, A_{psd} will be greater than 1and power spectral gain will be great.

3.2 Structural parameter setting rules of a and b

In order to analyze the influence of parameters a and b on the performance of larger parameter SR respectively, two experiments are conducted as follows:

(1) Setting b=1 and the response curve of A_{psd} in relation to a is gained and shown in Fig. 3(a).

(2) Setting a=0.1 and the response curve of A_{psd} in relation to b is gained and shown in Fig. 3(b).

Compared Fig. 3(a) with Fig. 3(b), it is found that A_{psd} begins to decline obviously after $a > 0.3$ and $b > 2$. In Fig. 3(a), decreases to 0 as a increase to 1. In Fig. 3(b), A_{psd} decreases to 0 as b increase to 10. That is to say, a makes a greater impact on A_{psd} than b. Therefore, the setting rule can be summarized as that a should be assigned in $(0, 0.3)$ and b in $(0, 2)$. For the sake of simplicity, b=1 is the assignment in this experiment.

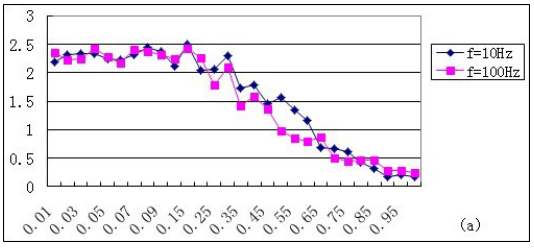

(a) The changing curve of A_{psd} with a

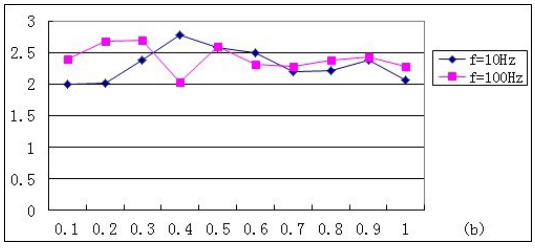

(b) The changing curve of A_{psd} with b

Fig. 3: The changing curve of A_{psd} with operation parameter at f=10Hz and f=100Hz

3.3 Noise parameter setting rules of D

When the SR system is used to extract the target signals, its anti-noise ability is a focus of most concern. The response curve of A_{psd} with D is shown in Fig. 4. A_{psd} decreases to 1 with a small slope as D increase from 0.5 to 10. Therefore, a conclusion can be drawn that the value

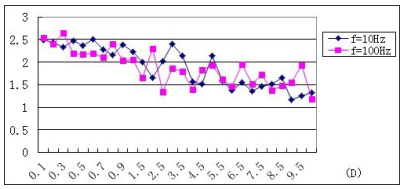

Fig. 4: The changing curve of A_{psd} with D at f=10Hz and f=100Hz

assignment of D has minimal impact on the anti-noise performance of SR system when sampling frequency of f_s, a and b values are assigned according the setting rules summarized above.

4 Experiment Results

4.1 Experimental data source

Rolling bearing type is $352226x2-2RZ$. Their main structural parameters are listed in Tab. 2. In the experiment, the bearing rotational speed is $500r/s$, the sampling frequency is 5120Hz and the acquisition time length is $20s$.

Table 2: Main technical parameters of the rolling bearing of $352226x2-2RZ$

the middle diameter D/mm	the diameter of roller d/mm	contact angle $\alpha/\circ$	The number of rollers z
176.29	24.74	8.833	20

4.2 The experiment results with the applications of the improved method

The paper mainly studies three kinds of typical faults of rolling bearings, such as inner ring surface damage, outer ring stripping injury and roller electrical erosion. Every test has just one fault. According to parameres in Tab. 2, the theoretical frequency value of three kinds of typical faults are calculated and shown in Tab. 3. In order to observe the experiment cures clearly, a data section of 4096 sampling point length is randomly cut out from the data package to calculate according to the improved method. The experimental results are shown in Fig. 5, Fig. 6, Fig. 7.

From Fig. 5 to Fig. 7, no feature can be seen in figure (a)(b)(c), while there is obvious peak in each figure (d). But a notice need to be emphasized is that frequency ranges of Fig. 5(d), Fig. 6(d) and Fig. 7(d) are all in $(0, 500)$Hz, because the spectrum energy concentrates here. According to informations in advance, the fault feature frequency of inner ring surface damage bulges at 70Hz, as the fault feature frequency of roller electrical erosion at 91Hz, and the fault feature frequency of the outer ring stripping injury at 30Hz. Comparing with the theoretical frequency value in Tab. 3, gaps between measured values and theoretical values are not big.

To sum up, through the Hilbert transform and SR system, obvious peak appears at the fault feature frequency in the figure of the output signal power spectrum of SR, noise power spectral

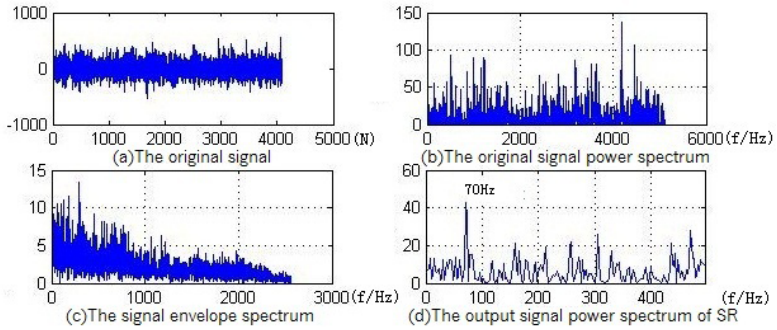

Fig. 5: Faults features extraction for surface damage of the inner ring

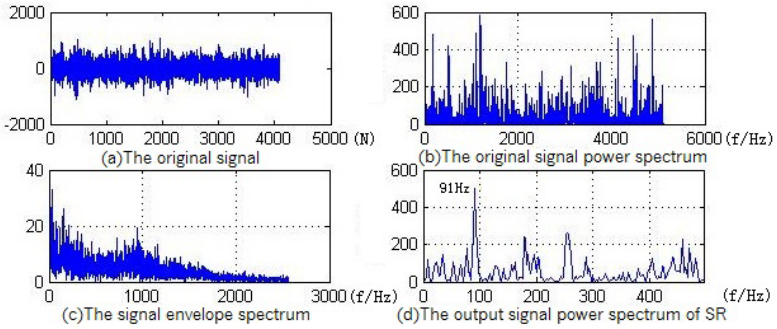

Fig. 6: Faults features extraction for surface damage of the inner ring

component evidently decreases, and signal-to-noise ratio (SNR) of the useful signal increases, which verify the feasibility of the proposed method.

4.3 Error analysis

Tab. 3 is the error analysis for three kinds of rolling bearing faults. It is easy to see from the fourth column that there is a small difference between the theoretical frequency value and the corresponding experiment measured one. The reasons for the errors can be summarized in two aspects. One is the parameters accuracy of the rolling bearing itself, such as geometry size error, not pure rolling of rolling element and so on. Another is outside factors, such as random measure error, noise and algorithmic calculation error. Because the errors in are all less than 5% and there are no other larger frequency values near the fault feature frequency, the errors don't affect its application in practice.

Table 3: Experiment error analysis

Fault type	Theoretical value $/Hz$	Measured value $/Hz$	Error
Inner ring surface damage	72.24	70	3.2%
Roller electrical erosion	95.5	91	4.9%
Outer ring stripping injury	29.31	30	2.3%

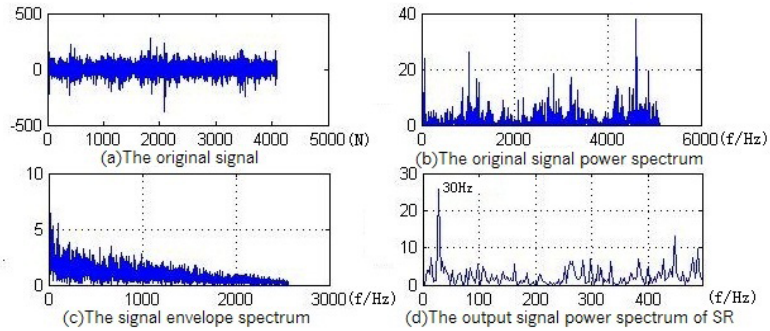

Fig. 7: Faults features extraction for surface damage of the inner ring

5 Conclusion

According to the simplified modulation model of the rolling bearing fault signal, an improved method with combination of Hilbert transform and the large parameter stochastic resonance algorithm is put forward and used to extracting fault features from test data. Firstly, Hilbert envelope detection algorithm is used to eliminate high frequency noise efficiently. Secondly, large parameter setting rules are summarized to overcome the limitation of the adiabatic approximation. Finally, improved method is applied to extract the fault features from the rolling bearing vibration signal and the experiment results have proved the effectiveness of the improved method. In addition to the research field of rolling bearing fault diagnosis, the method can be also applied to other rotating mechanical fault feature extraction, such as gears, rotors, shafts, etc.

References

[1] Junsheng Cheng, Dejie Yu, Rolling bearing fault diagnosis based on the analysis of the energy density, Journal of Vibration and Impact, 2001. 16 (3), pp. 79-81.

[2] Huahua Zhang, The signal enhancement algorithm based on optimal wavelet research and application, Electronic Test, 2010. 8, pp. 15-20.

[3] Tianyu Zhang, Nonlinear blind source separation based on neural network adaptive ICA algorithm research, Journal of Changchun University of Technology, 2010. 31 (3), pp. 334-339.

[4] Jianguo Chen, The mechanical fault feature extraction and classification method research based on independent component analysis, PhD Thesis, Dalian: Dalian university of technology, 2011.

[5] Cichocki Andrzej, Georgiev Pando, Blind Source Separation Algorithms with Matrix Constraints, IEICE Trans. Electronics, Communications and Computer Sciences, 2003. 86 (3), pp. 522-531.

[6] Gang Hu, Random force and nonlinear system, Shanghai Scientific Technology and Education Press, 1992

[7] Deli Liu, Yanbin Qu, Improved Hilbert-Huang transform in the application of electric power harmonica, Power system protection and control, 2012. 40 (06), pp. 69-73.

[8] Liangju Yi, Simple vibration diagnosis field practical technology, China Machine Press, 2003.

[9] Qiansheng Cheng, Digital signal processing (second edition), Peking University Press, 2010.

[10] Qiang Li, Taiyong Wang, et al, The weak signal detection technology based on variable step size stochastic resonance, Journal of Tianjin University, 2006. 39 (04), pp. 432-437.

[11] Baoguo Yang, Tan Tian, Bistable stochastic resonance system parameter selection algorithm and applications, Journal of Harbin Engineering University, 2011. 30 (03), pp. 432-437.